Acta Crystallographica Section D
Biological Crystallography
ISSN 0907-4449

Direct determination of the positions of the deuterium atoms of the bound water in concanavalin A by neutron Laue crystallography

Jarjis Habash,[a] James Raftery,[a] Rachel Nuttall,[a] Helen J. Price,[a] Clive Wilkinson,[b] A. Joseph Kalb (Gilboa)[c] and John R. Helliwell[a]*

[a]Section of Structural Chemistry, Department of Chemistry, University of Manchester, Manchester M13 9PL, England, [b]EMBL, F38042, Grenoble CEDEX, France, and [c]The Weizmann Institute of Science, Rehovot, Israel

Correspondence e-mail: john.helliwell@man.ac.uk

Received 7 October 1999
Accepted 8 February 2000

PDB Reference: concanavalin A, 1c57.

The correct positions of the deuterium (D) atoms of many of the bound waters in the protein concanavalin A are revealed by neutron Laue diffraction. The approach includes cases where these water D atoms show enough mobility to render them invisible even to ultra-high resolution synchrotron-radiation X-ray crystallography. The positions of the bound water H atoms calculated on the basis of chemical and energetic considerations are often incorrect. The D-atom positions for the water molecules in the Mn-, Ca- and sugar-binding sites of concanavalin A are described in detail.

1. Introduction

Concanavalin A is a saccharide-binding protein isolated from the jack bean and is the most thoroughly studied member of a class of proteins known as plant haemagglutinins or lectins [Kalb (Gilboa) *et al.*, 1999]. Its biological role is unknown, but it is thought to mediate cell–cell interactions by binding to polysaccharide on the cell surface. It also may have an anti-fungal plant-defence role. The molecule has a molecular weight of 25 kDa, contains 237 amino acids and binds a calcium and a transition metal ion, in this case Mn.

Structural studies by neutron diffraction permit elucidation of H/D exchange, which can yield vital information in understanding particular catalytic processes at the molecular level (for a general review, see Wlodawer, 1982). This approach exploits the difference in neutron-scattering lengths between H and D which is not present in X-ray diffraction. H atoms constitute a large proportion of any biological material and to understand the structure or the catalytic mechanism of such materials it is desirable to locate those atoms. Exchanging H for D in a neutron-diffraction experiment has three advantages. Firstly, reduction of the incoherent scattering by H is possible. Secondly, since D has a scattering length of 0.667, which is similar in sign and magnitude to those of the other atoms of the protein, whereas H has a scattering length of −0.374, this allows contrast-variation studies. Thirdly, deuteration also improves the location of water D atoms, as the scattering lengths of D and O are both positive in sign and the shape of the D_2O nuclear density indicates the D_2O orientation (Korszun, 1997). On the other hand, H and O have scattering lengths of opposite sign (H = −0.374 and O = 0.5805), resulting in partial cancellation of neutron bound water density at the diffraction resolutions typical of neutron protein crystallography (*i.e.* ∼2.5 Å). (For a review, see Savage & Wlodawer, 1986.) Clearly, then, a high level of D_2O exchange is important in a detailed study by neutron diffraction of the bound water in a protein crystal structure. Aside from the bulk water and water of hydration, which comprise

© 2000 International Union of Crystallography
Printed in Denmark – all rights reserved

approximately 50% of the crystal, the exchangeable atoms are those attached to N or O atoms, namely:

(i) all amides of the main-chain amino acids (except for prolines), *i.e.* the N—H bonds;

(ii) the side chains of Thr, Tyr, Asn, Ser, His, Lys, Arg, Trp and Gln with N—H or O—H bonds;

(iii) the side chains of Asp and Glu, if protonated in the first place.

The unexchangeable H atoms in the structure are those attached to C atoms, *i.e.* the C—H bonds.

In concanavalin A, there are 399 exchangeable H atoms and 1356 which are non-exchangeable. It should be noted that the large percentage of β-sheet in concanavalin A may hinder the H/D ratio of exchange in much of this protein (Wlodawer, 1982). Because of the opposite signs of the scattering lengths of H and D, partial exchange results in cancellation of the nuclear density and at an H/D ratio of 2:1 the nuclear density is rendered invisible. H/D exchange is discussed in more detail by Kossiakoff (1985).

The neutron Laue geometry harnesses a broader band of neutron wavelengths than a monochromatic beam and, with a very large image-plate detector, allows data collection in a reasonable time for smaller crystals and larger unit cells than in the past. Normally, months are required to record measurements from a single protein crystal sample in a neutron monochromatic beam. This was the case in an early neutron-diffraction study at 5 Å resolution of the cubic (space group $I2_13$, $a = 167.8$ Å) crystal of the complex of concanavalin A with perdeuterated methyl α-D-glucopyranoside [Yariv, Kalb (Gilboa) & Schoenborn, unpublished work]. Data collection can be reduced to a matter of days using the neutron Laue diffraction technique. Preliminary trials confirm that the large cubic crystals of the complex of concanavalin A with methyl α-D-glucopyranoside which we grow routinely in our laboratory (AJKG) are amenable to data collection in a reasonable time by means of the neutron Laue technique [Kalb (Gilboa), Habash, Helliwell & Myles, in preparation].

The synergy between synchrotron-radiation Laue and neutron Laue method developments has been described (Helliwell & Wilkinson, 1992; Helliwell, 1997). The first protein to be tested using the neutron Laue diffractometer ('LADI') at the ILL in Grenoble was a large triclinic crystal of lysozyme (Cipriani *et al.*, 1996). The unit-cell parameters were rather small and consequently this gave a strong diffraction pattern in just 2.50 h using a neutron white beam in the wavelength range 2.5–8.5 Å; diffraction data to 3 Å were recorded. Habash *et al.* (1997) studied deuterated concanavalin A (molecular weight 25 kDa *versus* 14.6 kDa for lysozyme) and obtained data to 2.75 Å using the neutron Laue method. Data collection took 11 d. Partial H/D exchange was accomplished by vapour diffusion. The atom on the carboxylic acid group of Asp28, of interest because it was shown in an ultra-high resolution X-ray experiment to form an Asp–Glu pair analogous to lysozyme's catalytic pair, was identified as an H atom, *i.e.* it had not exchanged for D under the vapour-diffusion conditions used. In the same year and using 'LADI', Niimura *et al.* (1997) investigated the structure of tetragonal hen egg-white lysozyme to 2 Å, for which data collection lasted 10 d. Their structure refinement identified 157 bound D_2O molecules, including D atoms on tightly bound D_2O molecules. Concanavalin A, with a unit-cell volume of 479 534 Å^3, yields only half the neutron-scattering intensity of tetragonal hen egg-white lysozyme of unit-cell volume 237 133 Å^3.

Very recently, the water arrangement in deuterated crystals of triclinic hen egg-white lysozyme was reported using quasi-Laue neutron diffraction (Bon *et al.*, 1999). The structure was analysed to 1.7 Å, with the location of 244 water molecules and the identification of the deuterated status of the H atoms in the protein.

Here, we present a structure of concanavalin A determined to the higher resolution of 2.4 Å, for which a more effective D_2O/H_2O exchange method was used. The X-ray structure at 1.8 Å of an identically prepared D_2O-exchanged concanavalin A crystal was also determined in order to provide as accurate as possible protein and bound water O atom positions. H atoms on the bound water O atoms were placed by the *X-PLOR* algorithm, which uses the nature, energetics and environment of these H atoms to calculate their positions. These (as D atoms) were then refined against the neutron Laue data whilst keeping the protein and bound water O atoms fixed at their X-ray positions.

2. Deuteration of the concanavalin A crystals

Large crystals of concanavalin A, grown by batch dialysis as described in Greer *et al.* (1970), were selected for the neutron study. These were transferred to a 1 ml portion of crystallization buffer made up in 99.9% D_2O (Aldrich) with 0.1 *M* $NaNO_3$, 0.05 *M* Tris–acetate, 1 m*M* $MnCl_2$, 1 m*M* $CaCl_2$, pH 6.5 (uncorrected glass-electrode reading) in a tightly sealed test tube. The D_2O solution was changed four times during the four-month soaking period.

The crystal form studied here is in space group *I*222. The chosen crystal, of dimensions $3 \times 2.5 \times 2$ mm (*i.e.* 15 mm^3), was mounted in a quartz capillary and used for neutron-diffraction data collection on the LADI diffractometer (Cipriani *et al.*, 1996) at the ILL. The large diameter of the capillary needed to hold the crystal required the strength of quartz over glass.

3. Data collection and analysis

Data were collected on the LADI diffractometer at the ILL, which exploited the neutron cold beam. The narrow bandpass of the neutron energies corresponding to a wavelength range of 2.49–3.52 Å was obtained using a multi-mirror bandpass filter comprising 40 Si-crystal mirrors each with 748 alternating 74–90 Å thick Ti and Ni layers. The shift towards shorter wavelength helps to enhance the resolution of the data (Habash *et al.*, 1997, used a 3–4 Å wavelength range, a concanavalin A crystal of dimensions $1.2 \times 1.8 \times 2.2$ mm and an exposure time of 11.5 h and achieved 2.75 Å resolution). A total of 20 neutron Laue images were collected from −60 to

Table 1
The number of reflections, completeness, R_{merge} and $I/\sigma(I)$ in resolution shells for the wavelength-normalized neutron Laue data.

Resolution (Å)	No. of reflections	Completeness (%)	R_{merge}	$I/\sigma(I)$
9.30	122	61.90	0.061	6.2
6.57	302	90.09	0.055	9.2
5.37	367	90.86	0.079	8.3
4.65	450	93.35	0.085	8.4
4.16	514	95.55	0.101	6.3
3.79	583	96.22	0.147	4.7
3.51	584	92.86	0.172	4.0
3.29	633	92.54	0.215	3.1
3.10	686	93.21	0.247	2.9
2.94	683	89.31	0.270	2.6
2.80	708	88.06	0.345	1.9
2.68	706	84.84	0.388	1.6
2.58	745	85.14	0.404	1.6
2.48	751	84.04	0.425	1.5
2.40	773	82.20	0.436	1.4

† $R_{merge} = \sum_h \sum_i |I_{hi} - \langle I_h \rangle| / \sum_h \sum_i \langle I_h \rangle$.

Table 2
Summary of X-ray data collection on an identically D_2O-soaked crystal.

(*a*) Data collection.

Data set	Crystal-to-detector distance (mm)	No. of images	Oscillation (°)	Exposure time (min)
1	87	132	1	30
2	140	47	1.5	15

(*b*) The number of reflections, completeness and R_{merge} in resolution shells.

Resolution (Å)	No. of reflections	Completeness (%)	R_{merge}
50.00–3.66	2858	99.2	0.048
3.66–2.91	2767	100.0	0.071
2.91–2.54	2767	100.0	0.093
2.54–2.31	2721	100.0	0.112
2.31–2.14	2704	100.0	0.132
2.14–2.02	2713	100.0	0.145
2.02–1.91	2719	99.6	0.163
1.91–1.83	2121	79.6	0.181
1.83–1.76	1611	59.2	0.218
1.76–1.70	1129	42.1	0.248

+54° in intervals of 6°. The exposure time per image was 23.5 h; 5 min was needed to scan the image plate and 1 min to erase it. The pixel size was 0.2 × 0.2 mm. For the eight 200 × 200 mm plates, a full scanned pattern comprised 4000 × 2000 pixels. The neutron Laue data were processed using the Daresbury Laboratory software developed for synchrotron Laue data processing (Helliwell *et al.*, 1989) but modified for neutron Laue data with a cylindrical detector geometry (diameter 318.3 mm; Campbell *et al.*, 1998). The orientation of the crystal was determined by autoindexing using the *LAUEGEN* program (Campbell, 1995), as was the prediction of the spots of each image. The unit cell was refined in *LAUEGEN* and the unit-cell parameters were a = 88.7, b = 86.5, c = 62.5 Å. The resolution limit was determined to be 2.4 Å. Reflections whose centres were closer than 2.3 mm were flagged as spatially overlapped but deconvoluted and then integrated. The *INTLAUE* program with the variable masks option was used for integration of each Laue reflection.

Table 3
Number of atoms in the structure.

Type	Number
H, unexchangeable	1356
H, exchangeable	399
C	1141
N	302
O	364
S	2
Mn	1
Ca	1
O waters	148
H waters, exchangeable	296

The *LAUENORM* program was used to derive the wavelength-normalization curve using the intensities of symmetry-equivalent reflections measured at different wavelengths. For a slightly truncated wavelength range of 2.65–3.35 Å, the Laue merging R factor for 40 420 normalized reflection-intensity measurements was 0.189. Merging these reflections in the *SCALA* program (Collaborative Computational Project, Number 4, 1994) produced an 88.49% complete unique set of 8605 reflections from these measurements, with an R_{merge} of 0.222. The statistics *versus* resolution are shown in Table 1.

This study to 2.4 Å resolution with D_2O exchange by direct soaking was compared with the earlier study to 2.75 Å which used the vapour-diffusion exchange method (Habash *et al.*, 1997) by scaling the data together using *SCALEIT* (Collaborative Computational Project, Number 4, 1994). The 4731 common reflections to 2.75 Å resolution gave a mean fractional difference ($R_{diff} = \sum_h |F_{PH} - F_P| / \sum_h |F_P|$) on F of 0.178 (weighted value 0.128). This indicates that there is a change in the ordered structure in the crystal anticipated to arise from the added scattering power owing to a larger proportion of H/D exchange.

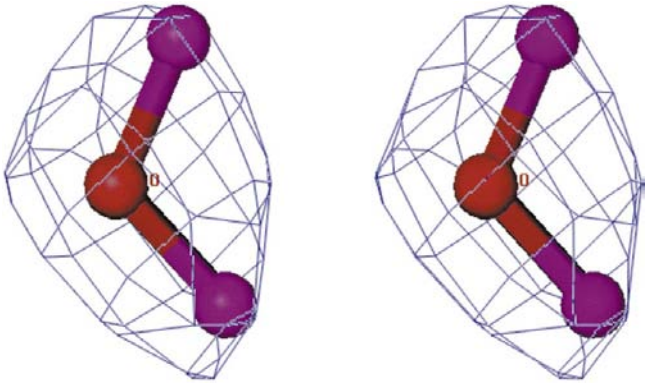

Figure 1
A water molecule (number 6 in the PDB file) in stereo showing the orientation of D_2O in the nuclear density (at 1.5σ).

4. X-ray model refinement

A crystal of concanavalin A of dimensions 1.6 × 0.95 × 0.5 mm deuterated under the same conditions as the crystal used for the neutron-diffraction measurements was used to collect X-ray data using our (Manchester) R-AXIS II area detector with Cu $K\alpha$ rotating anode radiation (λ = 1.5418 Å). Two data sets were collected, in slow and quick passes, in order to record data to higher and lower resolutions. Experimental data-collection details are shown in Table 2(*a*).

The data were processed in *DENZO* and merged in *SCALEPACK* (Otwinowski & Minor, 1997). The refined unit-cell parameters were a = 89.11, b = 87.58, c = 63.26 Å. The 24 110 unique reflections to 1.7 Å resolution were 88.1% complete and had an $R_{\rm merge}$ of 0.071; Table 2(*b*) gives the statistics for the data set *versus* resolution. As the starting structure, the coordinates from PDB file 1scs (Emmerich *et al.*, 1994) were refined by *X-PLOR* (Brünger, 1992) against all the X-ray data to 1.8 Å resolution to a final R factor (R factor = $\sum_h|F_{\rm obs} - F_{\rm calc}|/\sum_h|F_{\rm obs}|$) of 0.168 ($R_{\rm free}$ = 0.198 using 5% of data). In this X-ray model, H atoms (*i.e.* D atoms) were generated for the bound water O atoms according to the algorithm in *X-PLOR* (Brünger & Karplus, 1988).

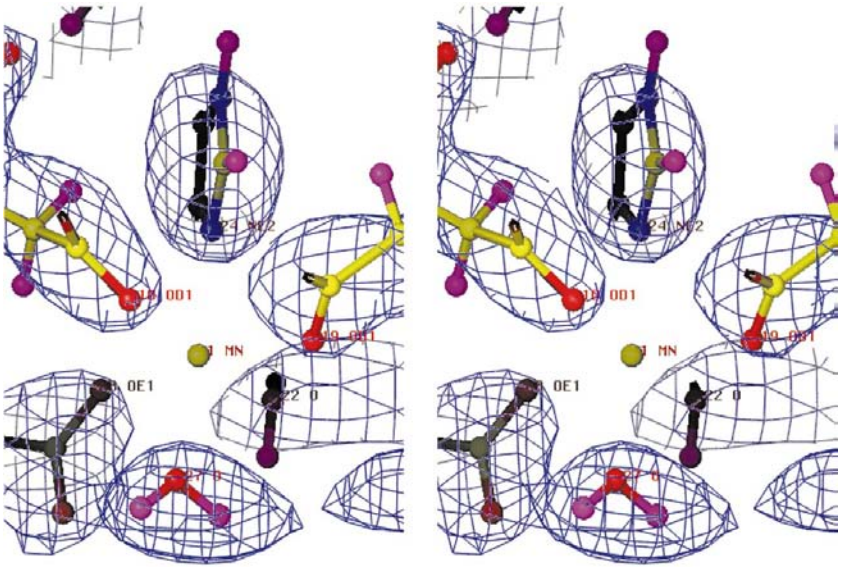

Figure 2
The $2F_o - F_c$ neutron-density map (at 1.5 r.m.s.) in stereo around the Mn coordination sphere of ligands.

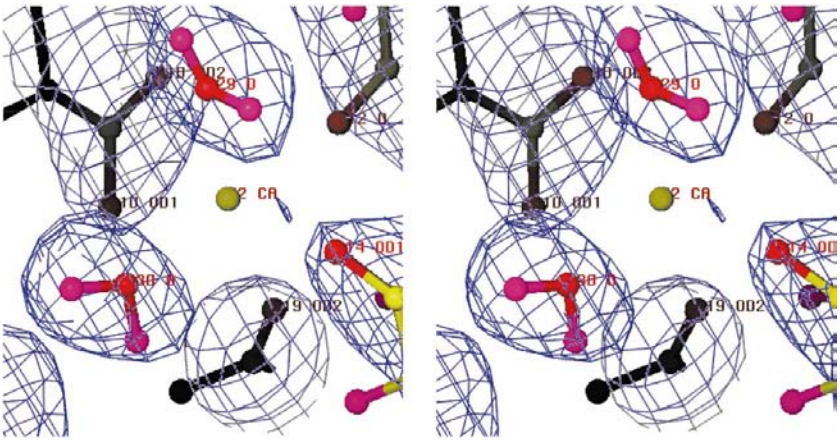

Figure 3
The $2F_o - F_c$ neutron-density map (at 1.5 r.m.s.) in stereo around the Ca coordination sphere of ligands.

5. Neutron structure refinement

The refined X-ray structure at 1.8 Å of a deuterated crystal determined as described in the previous section was used as the starting model for the neutron refinement using *X-PLOR* version 3.851 (Brünger, 1992). The structure, including the calculated H atoms, comprised 3566 protein atoms and 148 water molecules (see Table 3). The neutron-scattering lengths used throughout all the subsequent refinements were those of the Atomic Energy of Canada (1992) as shown in Table 4. The unit cell used was that determined by the Cu $K\alpha$ X-ray data reduction.

The first step was a 40-cycle rigid-body refinement using all neutron data to 2.4 Å. The maximum atom shift was 0.11 Å. The R factor dropped from 0.355 to 0.351. The $R_{\rm free}$ using 5% of the data dropped from 0.340 to 0.333. [It is odd that the $R_{\rm free}$ is less than the R factor at this step. Since the $R_{\rm free}$ subsets were different for the X-ray and neutron parts of the refinement, this might have been a bias effect. Subsequently, this was checked with the use of the same subsets, or at least those that were in the neutron data of the X-ray subset; the $R_{\rm free}$ and R factor were then 0.346 and 0.350, respectively, at this step (*versus* 0.333 and 0.351, respectively) and so a degree of bias is an explanation.]

This was followed by one trial of simulated annealing (SA), where the molecule underwent slow cooling from 1000 to 300 K in steps of 15 K, followed by 100 cycles of positional refinement. The positions of the bound water 'H atoms' (now D atoms) were of particular interest. As mentioned above, these 'H' atoms had been affixed in the final X-ray model to the bound water O atoms and then placed according to their neighbouring geometry *via* an algorithm in *X-PLOR*. The positions of these D atoms were refined against the neutron data with the rest of the model fixed. There were many cases where the initial H-atom positions were not in nuclear density, but after this refinement step the fit to the density was obviously correct. The R factor improved from 0.331 to

Table 4
Neutron-scattering lengths.

Atom type	Scattering length b (10^{-12} cm)
H	−0.374
D	0.667
C	0.665
N	0.936
O	0.580
S	0.285
Mn	−0.373
Ca	0.470

Table 5
Hydrogen-bonding network of the four waters liganded to Mn and Ca.

Donor	Neutron density (1.5σ)	Acceptor	D···O (Å)	O—D···O (°)
Water 27		Val32 O	2.10	141.9
	Connected	Glu8 OE2	2.65	79.3
Water 22		Ser34 OG	2.14	117.6
	Connected	Water 127 O	2.62	83.2
Water 29	Connected	Asp208 OD1	2.09	120.4
	Connected	Asp208 O	2.23	127.3
Water 30	Connected	Arg228 O	2.26	117.9

0.313, but R_{free} increased somewhat from 0.375 to 0.379. This was followed by 20 cycles of temperature-factor refinement with the exchangeable amide protons of the peptide bonds omitted (since the evaluation of their occupancy was undertaken later in the refinement). The R factor dropped from 0.311 to 0.245 and R_{free} dropped from 0.354 to 0.324. A bulk-solvent correction was applied and the temperature-factor refinement was repeated. The R factor decreased from 0.239 to 0.233 (R_{free} from 0.299 to 0.292).

H/D exchange on the N atoms and O atoms was then investigated by comparing several models; firstly assuming all had exchanged to D from H, secondly that none had exchanged, thirdly that no H or D was assumed (*i.e* 2/3rds and 1/3rd exchange model for H and D, respectively) and fourthly actual occupancy refinement was undertaken. In terms of the R_{free} and the R factor the lowest *i.e.* best values were 0.292 and 0.233, respectively, for the third model. For the best (third) model, a further ten cycles of positional refinement of the 148 D_2O molecules were performed while keeping the protein and the two metal atoms fixed. The R_{free} and R factor were reasonably stable at 0.301 and 0.270, respectively, indicating that convergence had been reached. This also provided a sensitivity check on the X-ray-derived water O-atom positions. Using *LSQKAB* (Collaborative Computational Project, Number 4, 1994), the two models were superimposed and the bound water average displacements calculated. The average displacement over the 444 bound water atoms was 0.04 Å. The worst shift was water 136 O with a shift of 0.4 Å; this atom had a B factor of 47 and is not featured in metal- or sugar-binding roles. For the latter subset of waters 22, 27, 29, 30, 31, 33 and 34, the shifts for the O atoms were 0.05, 0.03, 0.04, 0.03, 0.03, 0.07 and 0.05 Å, respectively. For water 6, featured in Fig. 1, the O-atom shift was 0.03 Å. Although the R factor had risen slightly, this model has the merit of finally being a neutron-only refined model for the bound water. $F_o - F_c$ and $2F_o - F_c$ neutron-density maps were then calculated for this final model. The maps were read into the *O* graphics computer program (Jones *et al.*, 1991) and contoured to show positive and negative nuclear density. Residue-by-residue inspection of the $2F_o - F_c$ maps showed that the model fitted the positive nuclear density for those atoms scattering positively and fitted negative nuclear density for those scattering negatively, *i.e.* most H atoms attached to C atoms.

Owing to a high percentage of β-sheet in the structure, the elaboration of H/D exchange in the peptide chain proved not to be straightforward. In order to undertake this, the output model of the final cycle of *X-PLOR* neutron

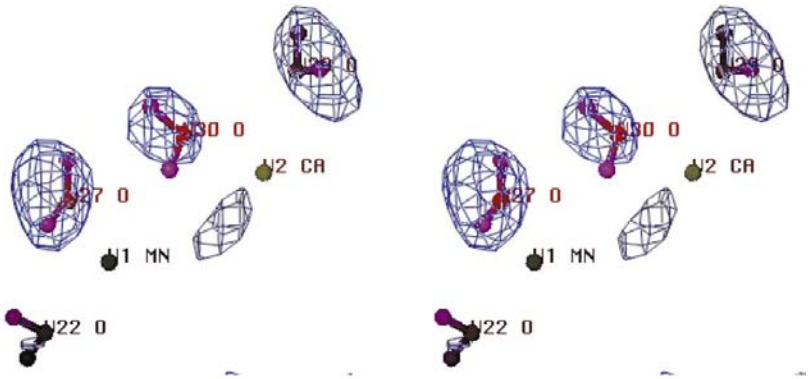

Figure 4
The $F_o - F_c$ neutron omit map in stereo showing the four waters (at 3σ) linked to Mn and Ca coordination.

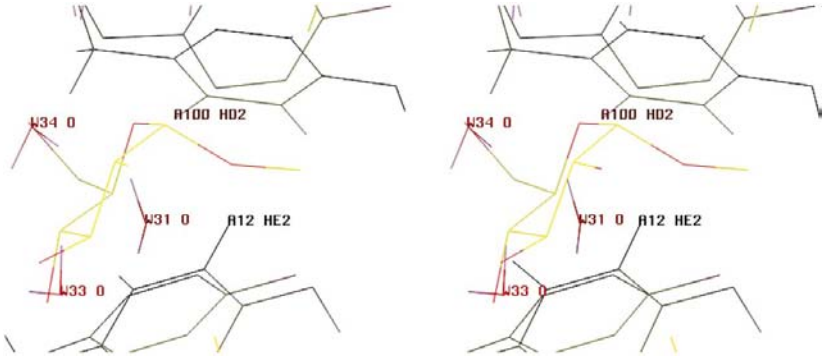

Figure 5
The saccharide-binding site in stereo showing the sugar-free structure (from this work) and, superimposed on it, a model of glucose-bound concanavalin A (the latter from Bradbrook *et al.*, 1998).

Table 6
The Mn coordination-sphere ligands.

Mn—ligand	Distance (Å)
Mn—OE1 (Glu8)	2.19†
Mn—OD1 (Asp10)	2.17†
Mn—OD1 (Asp19)	2.24†
Mn—NE2 (His24)	2.28†
Mn—O (water 22)	2.17
Mn—O (water 27)	2.28

† These distances are derived from the X-ray refinement of the D_2O-soaked crystal.

Table 7
The Ca coordination-sphere ligands.

Ca—ligand	Distance (Å)
Ca—OD1 (Asp10)	2.47†
Ca—OD2 (Asp10)	2.48†
Ca—O (Tyr12)	2.34†
Ca—OD1 (Asn14)	2.36†
Ca—OD2 (Asp19)	2.44†
Ca—O (water 29)	2.42
Ca—O (water 30)	2.38

† These distances are derived from the X-ray refinement of the D_2O-soaked crystal.

refinement was input to *SHELXL* (Sheldrick & Schneider, 1997) for occupancy refinement. To determine the extent of H/D exchange of the N—H amides on the protein (228 atoms), the occupancy of each exchangeable H was tied to the occupancy of a D using the 'free-variable facility' so that the sum of their occupancies was constrained to be equal to 1.0. After 30 cycles of refinement, the R factor converged to 0.243 ($R_{\rm free}$ = 0.296). The occupancies of H and D varied from 0 to 1.0 for most of the peptides. A few occupancies exceeded 1.0. From the fractional occupancies of H and D, it is clear that the degree of exchange was variable along the peptide chain. $2F_o - F_c$ maps produced at this stage were similar to the final maps produced with *X-PLOR*, *i.e.* no special advantage seemed to accrue for the H/D occupancy refinement over that for which the 2/3rds and 1/3rd occupancy model was made.

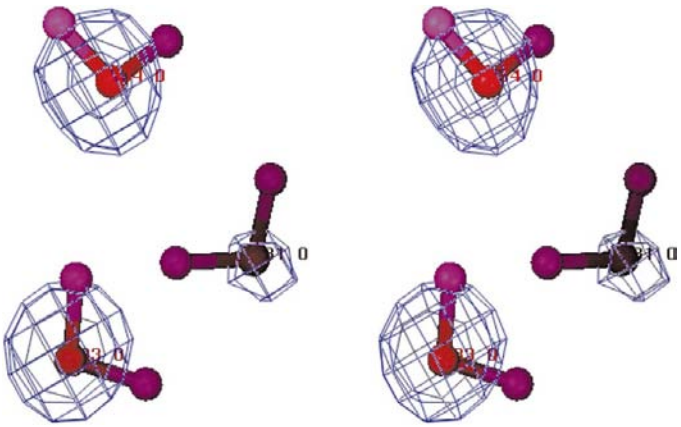

Figure 6
The $2F_o - F_c$ X-ray map (1.5σ) in stereo showing the three waters at the saccharide-binding site.

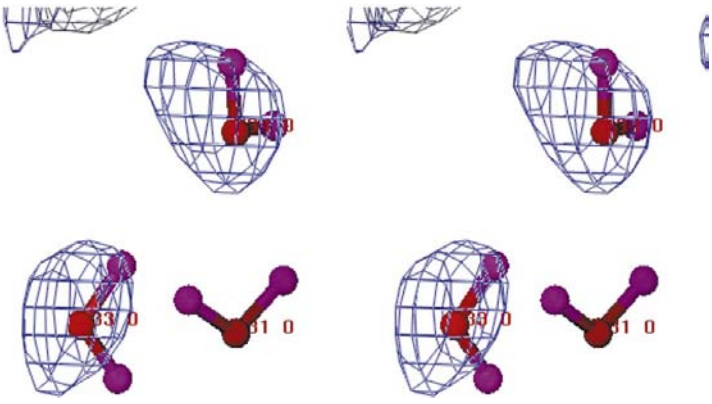

Figure 7
The $F_o - F_c$ X-ray omit map (at 3σ) in stereo for the three waters at the saccharide-binding site.

6. The bound water structure

There are 148 bound water molecules to be investigated. Many waters appear as D_2O, *i.e.* with elongated positive density in the $2F_o - F_c$ map. The water D atoms are thereby important contributors to the overall scattering. There are many examples where the initial H-atom positions assigned by *X-PLOR* to the X-ray model were not in nuclear density, but after refinement against the neutron data the fit to the density was obviously correct. These are waters that are hydrogen-bond donors or acceptors either with the protein or with other water molecules, *e.g.* in water clusters. Fig. 1 is a stereo diagram of a well ordered water molecule D_2O where the O atom and its two D atoms enhance each other to give positive neutron density with a shape evident for the nuclear density.

Two water molecules (numbered 22 and 27 in the PDB file associated with this paper) are coordinated to the Mn atom in the transition metal-binding site and another two water molecules (29 and 30) are coordinated to the Ca atom in the nearby calcium-binding site. These are shown in Figs. 2 and 3. When an omit map was produced for these four metal-coordinated water molecules, three waters (27, 29 and 30) appeared at 3σ, but water 22 was weak, appearing at 1.5σ. Fig. 4 shows this omit map.

This work was extended by calculating an omit map for the eight D atoms of the four metal-coordinated waters. The four D atoms of waters 27 and 29 appeared clearly at the 3σ contouring level. At 1.5σ, more D atoms appeared, but water 22 showed one D atom only. Table 5 shows tabulated values for the hydrogen bonds formed by the four water molecules in terms of donor and acceptor. In all the waters, the O—D1 and O—D2 distances are constrained to be 1 Å.

Of the 148 defined bound waters, 93 are in the primary hydration shell and 55 are in the secondary hydration shell. In the primary hydration shell, 53 bound waters

Table 8
Mn and Ca distances to D atoms of waters.

Mn/Ca—D	Distance (Å)
Mn—D1 (water 22)	2.87
Mn—D2 (water 22)	2.63
Mn—D1 (water 27)	3.08
Mn—D2 (water 27)	2.77
Ca—D1 (water 29)	2.69
Ca—D2 (water 29)	3.32
Ca—D1 (water 30)	3.24
Ca—D2 (water 30)	2.75

Table 9
Bound water comparison for the 2.4 Å neutron room-temperature structure (this work) and 0.94 Å X-ray cryo-structure (Deacon *et al.*, 1997).

	Total No. of waters	Common waters (within 1 Å)	D_2O	D—O	H_2O	H—O
Neutron structure	148					
X-ray structure	319					
		88				
			62	20		
					12	35

have nuclear density corresponding to D_2O, 14 to D—O, one to O only and 25 have no nuclear density (at 1.5 r.m.s.). In the secondary hydration shell, the corresponding numbers are 35, 8, 0 and 12, respectively. Since water can behave as a hydrogen-bond donor as well as an acceptor (to the oxygen lone pairs), for 88 observed D_2O and 22 D—O there are 396 ($4 \times 88 + 2 \times 22$) potentially observable (non-bifurcated) hydrogen bonds. The ideal hydrogen-bond angle for O—D$\cdots A$ (where A is an acceptor) is 180°; in this study, 153 hydrogen bonds have O—D$\cdots A$ angles greater than 100°; it is assumed that in a hydrogen bond the bound water D atom to acceptor atom distance is also less than 3 Å. As an acceptor, the D—O$\cdots$D bond angle is considered to be 109°. There are 62 hydrogen bonds with D—O$\cdots$D angles in the range 90–130°. Together (donor plus acceptor situations), these comprise 215 of the 396 potentially observable hydrogen bonds.

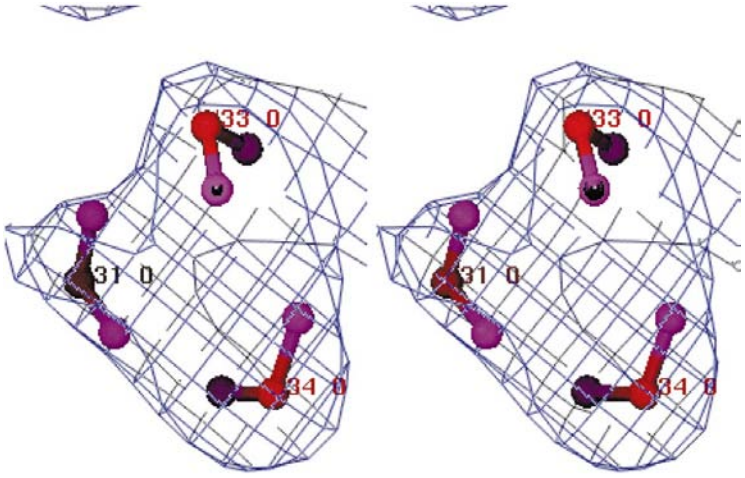

Figure 8
The $2F_o - F_c$ neutron map (1.5σ) in stereo showing the three waters at the saccharide-binding site.

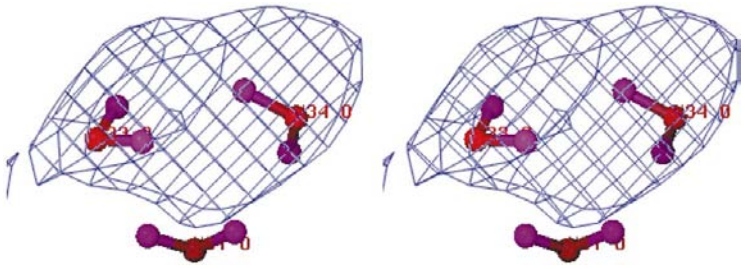

Figure 9
The $F_o - F_c$ neutron omit map (at 3σ) in stereo for the three waters at the saccharide-binding site.

7. The metal sites

The transition metal manganese is coordinated to Glu8, Asp10, Asp19, His24 and two D_2O water molecules. The neutron-scattering length for Mn is −0.373 (essentially the same as the scattering length of H) and is observable in the negative density $2F_o - F_c$ map. In X-ray scattering, $(Z_H)^2/(Z_{Mn})^2$ is 0.0016, but in neutron diffraction $(b_H)^2/(b_{Mn})^2$ is 1.0058. The transition-metal site is largely occupied by Mn. Metal atoms other than Mn which may bind to the site are Co, Ni, Zn and Cd. Their neutron-scattering lengths are 0.249, 1.030, 0.568 and 0.487, respectively. If present, these would tend to cancel the negative density of Mn. Partial occupancy by metals other than Mn is low to zero in the crystal, as deduced from results of an Mn MAD experiment study of native concanavalin A (Hunter *et al.*, 1999).

Calcium is coordinated to Asp10 (both OD1 and OD2), Tyr12, Asn14, Asp19 and two water molecules. The neutron-scattering length for Ca is 0.490, which as expected shows positive density in the $2F_o - F_c$ map. The distances of Mn and Ca from their ligands as determined in this study (by the X-ray refinement) are shown in Tables 6 and 7, respectively. Here also, $(Z_H)^2/(Z_{Ca})^2$ is 0.0025 for X-ray diffraction, but $(b_H)^2/(b_{Ca})^2$ is 0.5824 for neutron diffraction. Figs. 2 and 3 show the metals coordinated to their ligands; the interesting feature is the positioning of the D_2O in the neutron density, where the O atoms point toward the metals and the D atoms point away (see Table 8).

8. The saccharide-binding site

The saccharide-binding site is shown in Fig. 5. In the saccharide-free crystal form studied here, the saccharide-binding site is occupied by three water molecules; they form hydrogen bonds to the protein similar to those formed by the hydroxyl

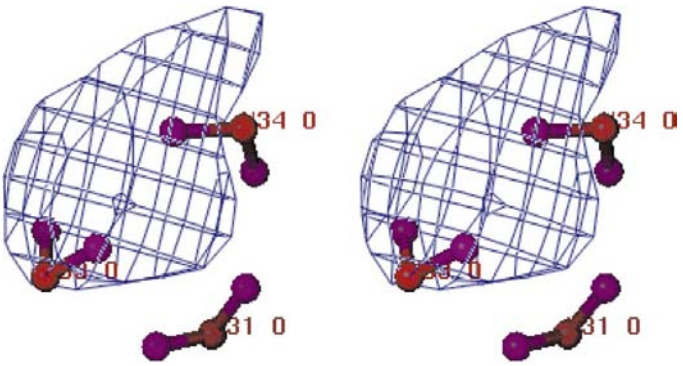

Figure 10
The $F_o - F_c$ neutron omit map (at 3σ) in stereo for the six D atoms of the three waters at the saccharide-binding site.

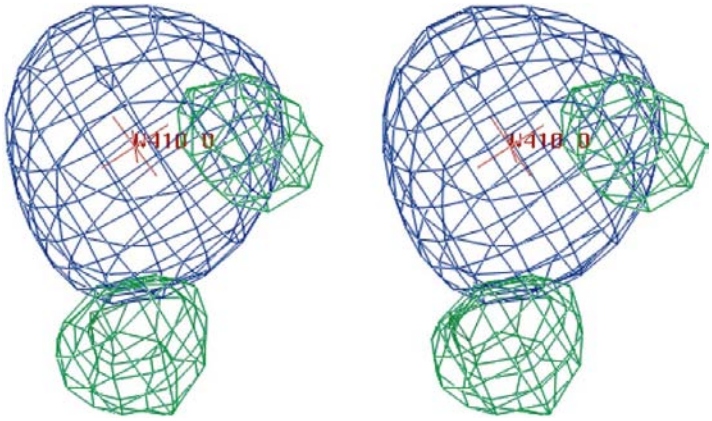

Figure 11
The $2F_o - F_c$ 0.94 Å X-ray omit map (in blue at 2.7 r.m.s.) overlaid on the $F_o - F_c$ 0.94 Å X-ray omit map (in green at 1.8σ) in stereo showing an H_2O molecule (water 410).

groups of bound saccharide. X-ray derived maps were produced for comparison with neutron maps in order to investigate these waters and their D atoms in detail. In the $2F_o - F_c$ X-ray map contoured at 1.5 r.m.s., the three waters (34, 33 and 31) are spherical in shape as expected considering the insignificant contribution of D atoms to the X-ray diffraction. Waters 34 and 33 were clearly visible and water 31 less so, as shown in Figs. 6 and 7.

The final neutron model also shows the three deuterated waters (34, 33 and 31) in the final $2F_o - F_c$ map. These waters cluster together to form continuous neutron density at 1.5σ. In the $F_o - F_c$ omit map at 3σ, waters 34 and 33 are clearly visible, while water 31 is without density (see Figs. 8 and 9). Of the six D atoms of the three waters 34, 33 and 31, three of these are visible at 3σ, *i.e.* those associated with waters 33 and 34. Fig. 10 shows this difference map for the neutron data (at lower σ levels more D atoms appear). These three waters are solidly seen in $2F_o - F_c$ maps even when contoured at the 2 r.m.s. level. Water 31 is hydrogen bonded to both water 33 and water 34. It is probable that water 33 is hydrogen bonded to water 34 and thus the three waters are linked in a triangular manner. These waters fill the binding site snugly and water 33 and 34 form hydrogen bonds to the adjacent protein. Water 33 donates D to form a hydrogen bond to Asp208 OD1, while its O atom can form a hydrogen bond to the adjacent Asn14 HD22. Water 34 is close enough to form hydrogen bonds to Tyr100 HN and Asp208 OD2.

Bradbrook *et al.* (1998) have discussed in detail the O atoms of a bound monosaccharide (glucose) and their hydrogen bonds to Leu99 NH, Tyr100 NH, Asp208 OD1 and OD2, Arg228 NH and Asn14 ND2. In the X-ray D_2O structure, the two water O atoms of water 33 and 34 superimpose well onto two of the sugar's O atoms in the complexes of glucoside concanavalin A. The third O atom (water 31) is farther away and therefore this eliminates the likelihood of any contacts with Leu99 and Arg228, as made by the sugar oxygen, for this water.

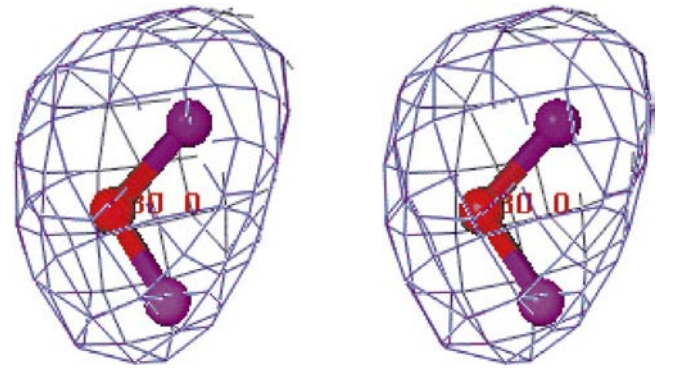

Figure 12
The $2F_o - F_c$ neutron map (1.5 r.m.s.) in stereo showing a D_2O molecule (water 30) (see also Fig. 1).

9. Comparison of the neutron structure at 2.4 Å with the X-ray high-resolution 0.94 Å structure

The neutron structure at room temperature and the X-ray ultra-high resolution (0.94 Å) structure at 110 K reported previously (Deacon *et al.*, 1997) were superimposed by means of the program *LSQKAB* (Collaborative Computational Project, Number 4, 1994) in order to evaluate the effectiveness of each method in determining the positions of bound water H/D atoms.

The nuclear density $2F_o - F_c$ map (contoured at 1.5 r.m.s.) was compared with the 0.94 Å X-ray $2F_o - F_c$ map generated by *SHELXL* (contoured at 2.7 r.m.s.) and the 0.94 Å X-ray $F_o - F_c$ difference map (contoured at 1.8σ). A total of 88 bound water O atoms were found to coincide (within 1 Å) for the two structures (see Table 9). Other common waters may occur below 1.5 r.m.s. in the nuclear-density map, but were not included. Of these 88, 62 could be assigned as D_2O, 20 showed only one D atom and six showed either poor density or the

molecule was not properly oriented in the neutron density. This compares with the ultra-high resolution X-ray study, where there are 12 water molecules with both H atoms visible, 35 with only one visible and 41 where no H atom is visible (see Table 9). Figs. 11, 12, 13 and 14 show the comparison of protonated and deuterated waters as examples.

Neutron diffraction is clearly more efficient than X-ray diffraction for determining H/D-atom positions, *i.e.* it yields the largest number. The best agreement between the two structures is obtained when comparing the four waters liganded to Mn and Ca atoms and the three waters at the sugar-binding site. For the four waters at the Mn and Ca sites, eight D atoms out of eight were visible in the neutron study and four protons were found in the ultra-high resolution X-ray study (here, waters 27 and 29 with H atoms and the other two without H atoms).

At the sugar-binding site only one proton is visible from the 0.94 Å X-ray study, whereas in the current neutron-diffraction study four of the six water D atoms are visible even though the resolution limit is much poorer. Obviously, the 0.94 Å ultra-high resolution X-ray approach does yield bound water H atoms more accurately than this 2.4 Å neutron-diffraction study. (Clearly, if *e.g.* 1.5 Å neutron-diffraction data could be collected then this may favour the neutron diffraction over the 0.94 Å X-ray study.)

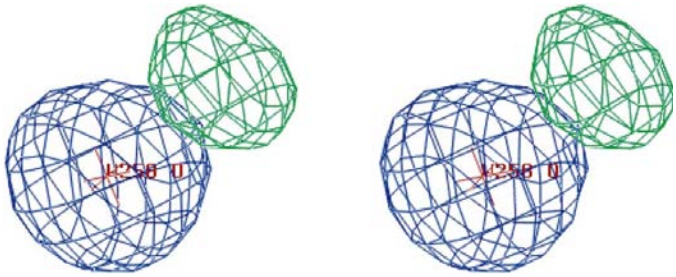

Figure 13
The $2F_o - F_c$ 0.94 Å X-ray omit map (in blue at 2.7 r.m.s.) overlaid on the $F_o - F_c$ 0.94 Å X-ray omit map (in green at 1.8σ) in stereo showing the H—O of water 258.

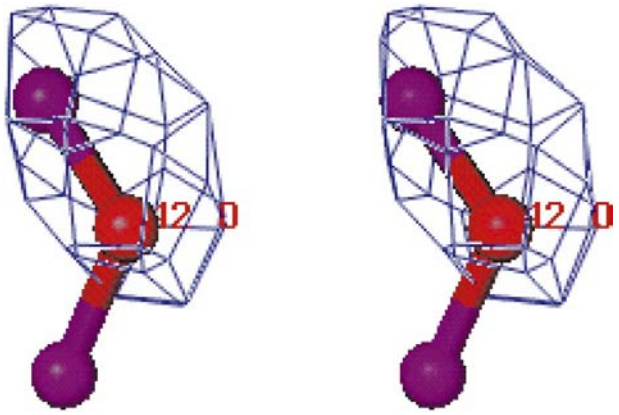

Figure 14
The $2F_o - F_c$ neutron map (1.5 r.m.s.) in stereo showing the D—O of water 42.

10. Conclusions

This neutron Laue study has allowed the definition of the nature of the Mn ligand environment and interrelates with an EPR spectroscopic study [AJK(G)] for which the coordinates of the H/D atoms of the two water molecules in the ligation sphere of the Mn are necessary for the interpretation of the spectra. This neutron study has revealed directly that the two bound waters' D atoms are indeed pointing away from the Mn atom. Comparing results from this D_2O *versus* partially D_2O exchanged crystal of Habash *et al.* (1997), the bound solvent now is much richer in detail, whereas before the bound water molecules had essentially zero density (at 2.75 Å resolution). The extensive direct soaking of the crystal in D_2O has yielded the D-atom positions of the bound water molecules. The reduction of the number of H atoms *via* this D_2O soaking method has also enhanced the neutron-diffraction resolution, presumably *via* a reduction of the hydrogen background scattering.

The positions of the bound water D atoms, placed according to their environment *via* an algorithim applied by *X-PLOR*, were often incorrect. Neutron diffraction of the bound water D_2O molecules, even at the relatively low resolution of this study, is seen to be more attractive than ultra-high resolution X-ray diffraction in assigning many more coordinates of the D-atom positions in bound D_2O; some 62 D_2O molecules were revealed and 20 with one D atom were visible and at room temperature. For the bound water in the ultra-high resolution X-ray case, there are rather few of these (12 H_2O molecules, 35 with one H atom visible, out of 319) even at 110 K. However, these few are rather well determined. The complementarity of the neutron and X-ray approaches is thus evident. For the particular case of the saccharide-binding site of concanavalin A, this neutron study has revealed the bound waters' D atoms at that binding site. As a sugar ligand approaches the receptor-binding site on the protein the mutual orientation of these waters together is now known. This is a new level of detail for molecular-recognition and molecular-modelling studies in the future. Predicting binding affinity of ligands is very difficult, as recent examples show (Bradbrook *et al.*, 1998; Davies *et al.*, 1999). The structural definition of bound water molecules in a ligand site is improved *via* neutron Laue diffraction studies, as exemplified here and need not be neglected in molecular-modelling studies in the future.

The Wellcome Trust is thanked for funding JH in a research grant award to JRH. The ILL is thanked for the provision of neutron beam time and subsistence at the ILL during data collection. We warmly thank Dr Mogens S. Lehmann for discussions. The BBSRC is thanked for the purchase of Silicon Graphics computer workstations and molecular graphics and partial salary support for JR. The British Council funded HJP *via* a PhD studentship under a UK/Israel Collaborative Science award to JRH and AJK(G).

References

Atomic Energy of Canada (1992). *Neutron News*, **3**, 29–37.

Bon, C., Lehmann, M. S. & Wilkinson, C. (1999). *Acta Cryst.* D**55**, 978–987.

Bradbrook, G. M., Gleichmann, T., Harrop, S. J., Habash, J., Raftery, J., Kalb (Gilboa), J., Yariv, J., Hillier, I. H. & Helliwell, J. R. (1998). *J. Chem. Soc. Faraday Trans.* **94**(11), 1603–1611.

Brünger, A. T. (1992). *X-PLOR Version* 3.1: *A System for X-ray Crystallography and NMR.* New Haven, CT, USA: Yale University Press.

Brünger, A. T. & Karplus, M. (1988). *Proteins Struct. Funct. Genet.* **4**, 148–156.

Campbell, J. W. (1995). *J. Appl. Cryst.* **28**, 228–236.

Campbell, J. W., Hao, Q., Harding, M. M., Nguti, N. D. & Wilkinson, C. (1998). *J. Appl. Cryst.* **31**, 496–502.

Cipriani, F., Castagna, J.-C., Wilkinson, C., Oleinek, P. & Lehmann, M. S. (1996). *J. Neutron Res.* **4**, 79–85.

Collaborative Computational Project, Number 4 (1994). *Acta Cryst.* D**50**, 760–763.

Davies, T. G., Hubbard, R. E. & Tame, J. R. H. (1999). *Protein Sci.* **8**, 1432–1444.

Deacon, A., Gleichmann, T., Kalb (Gilboa), A. J., Price, H., Raftery, J., Bradbrook, G., Yariv, J. & Helliwell, J. R. (1997). *J. Chem. Soc. Faraday Trans.* **93**(24), 4305–4312.

Emmerich, C., Helliwell, J. R., Redshaw, M., Naismith, J. H., Harrop, S. J., Raftery, J., Kalb (Gilboa), A. J., Yariv, J., Dauter, Z. & Wilson, K. S. (1994). *Acta Cryst.* D**50**, 749–756.

Greer, J., Kaufman, H. W. & Kalb, A. J. (1970). *J. Mol. Biol.* **48**, 365–366.

Habash, J., Raftery, J., Weisgerber, S., Cassetta, A., Lehmann, M. S., Hoghoj, P., Wilkinson, C., Campbell, J. W. & Helliwell, J. R. (1997). *J. Chem. Soc. Faraday Trans.* **93**(24), 4313–4317.

Helliwell, J. R. (1997). *Nature Struct. Biol.* **4**(11), 874–876.

Helliwell, J. R., Habash, J., Cruickshank, D. W. J., Harding, M. M., Greenhough, T. J., Campbell, J. W., Clifton, I. J., Elder, M., Machin, P. A., Papiz, M. Z. & Zurek, S. (1989). *J. Appl. Cryst.* **22**, 483–497.

Helliwell, J. R. & Wilkinson, C. (1992). *HERCULES: Higher European Research Course for Users of Large Experimental Systems*, Vol III, pp. 212–217.

Hunter, N. S., Gleichmann, T., Helliwell, M., Barba, L., Busetto, E., Lausi, A., Price, H. J. & Helliwell, J. R. (1999). *Croatia Chem. Acta*, **72**(2–3), 673–684.

Jones, T. A., Zou, J. Y., Cowan, S. W. & Kjeldgaard, M. (1991). *Acta Cryst.* A**47**, 110–119.

Kalb (Gilboa), A. J., Habash, J., Hunter, N. S., Price, H. J., Raftery, J. & Helliwell, J. R. (1999). *Metal Ions in Biological Systems*, Vol. 37, *Manganese and Its Role in Biological Processes*, edited by A. Sigel & H. Sigel, pp. 279–300. New York: Marcel Dekker Inc.

Korszun, Z. R. (1997). *Methods Enzymol.* **276**, 218–232.

Kossiakoff, A. A. (1985). *Annu. Rev. Biochem.* **54**, 1195–1227.

Niimura, N., Minezaki, Y., Nonaka, T., Castagna, J.-C., Cipriani, F., Hoghoj, P., Lehmann, M. S. & Wilkinson, C. (1997). *Nature Struct. Biol.* **4**(11), 909–914.

Otwinowski. Z. & Minor, W. (1997). *Methods Enzymol.* **276**, 307–326.

Savage, H. & Wlodawer, A. (1986). *Methods Enzymol.* **127**, 162–183.

Sheldrick, G. M. & Schneider, T. R. (1997). *Methods Enzymol.* **277**, 319–343.

Wlodawer, A. (1982). *Prog. Biophys. Mol. Biol.* **40**, 115–159.